Hindawi Publishing Corporation
Shock and Vibration
Volume 2016, Article ID 9425273, 8 pages
http://dx.doi.org/10.1155/2016/9425273

Research Article

Optimum Operating Conditions of $(Pb_xX_{1-x})(Zr_yTi_zY_{1-y-z})$ Piezoelectric Transducer for Vibrational Energy Harvesting Applications

Funda Demir[1] and Mustafa Anutgan[2,3]

[1] *Electronics Technology Department, Karabuk University, 78050 Karabuk, Turkey*
[2] *Mechatronics Engineering Department, Faculty of Technology, Karabuk University, 78050 Karabuk, Turkey*
[3] *Thin Film Coatings Laboratory, Materials Research and Development Center (MARGEM), Karabuk University, 78050 Karabuk, Turkey*

Correspondence should be addressed to Funda Demir; fundademir@karabuk.edu.tr

Received 4 July 2016; Accepted 9 November 2016

Academic Editor: Tony Murmu

The electrical energy production capability of bimorph $(Pb_xX_{1-x})(Zr_yTi_zY_{1-y-z})$ fiber composite piezoelectric transducer has been investigated for energy harvesting applications. The material has been analyzed under different frequencies, bending amounts, and temperatures. The operating conditions for maximum electrical energy outcome have been determined. The natural frequencies of oscillations in the macro dimensions have been found to be inversely proportional to the length of the material. On the other hand, the voltage output with respect to the oscillation frequency exhibits an interesting behavior such that the characteristic curve shifts to higher frequencies as the bending radius is decreased. This behavior has been interpreted as a result of possible overtone transitions of the oscillations to a stiffer mode. The increasing temperature has been observed to have a negative effect on the piezoelectric energy harvesting property. When the determined optimum conditions were utilized, the amount of electrical energy stored in 6300 s by an energy harvester circuitry has been found to be 0.8 J.

1. Introduction

As the environmental concerns and limited resources decrease the popularity of the traditional energy production methods, clean and renewable techniques using solar, wind, geothermal, wave, and vibrational energies gain more importance [1–5]. Among these, energy harvesting from vibrations is promising especially for μW applications as it renders relatively high energy densities.

Various principles utilized to transform vibrational energy into electrical energy can be cited as electromagnetism, electrostatics, and piezoelectricity. When compared with the formers, piezoelectricity leads to about 3 times greater energy density output [6, 7]. Furthermore, the power obtained in the μW scales when a piezoelectric material is operated under ordinary conditions can be improved toward mW scales via proper optimization procedures. These procedures include [8–10]

(i) the use of different materials such as lead zirconate titanate ($(Pb_xX_{1-x})(Zr_yTi_zY_{1-y-z})$ or (PZT)), polyvinylidene fluoride (PVDF), and macrofiber composite (MFC);

(ii) loading the piezoelectric material in directions parallel (d31) or perpendicular (d33) to the plane of electrodes;

(iii) the choice of geometrical shape (ring, triangle, square, etc.) of the piezoelectric material;

(iv) the production of the material in different types of morphology (unimorph, bimorph, s-morph, etc.);

(v) the design of the energy harvester circuitry of AC-DC rectifier (half-wave, full-wave, and bridge), DC-DC converter (buck, boost, and buck-boost), and the storage device (rechargeable battery, super capacitor, etc.).

On the other hand, brittleness of the piezoelectric materials may be regarded as their main disadvantage [11].

Among piezoelectric materials, PZT piezoceramic transducer has a high reputation [12–15]. Its piezoelectric charge coefficient (d), piezoelectric voltage coefficient (g), dielectric constant (ϵ), electromechanical coupling coefficient (k), and charge sensitivity are high, whereas its mechanical loss is low [16, 17]. Recent works regarding the PZT transducer mostly focus on ultrasonography technology and acoustic microscopy owing to its suitable physical properties [18]. Consequently, PZT transducer, which is capable of working over 30 MHz, is used in different branches like dermatology, intravascular, intracochlear implants [19–21], displays [22], and other optoelectronics devices [23–28] integrated with micro electromechanical systems (MEMS), micro spectroscopy [28–30], optical coherence tomography [31–35], microfluidity applications [36], electromechanical impedance (EMI) spectroscopy for real-time monitoring [37], biosensors sensitive at nanoscales [38], radio frequency (RF) applications [39], and lens-on-silicon ultrasound focusing units [40]. Furthermore, PZT thin film high frequency (~100 MHz) transducers were also studied well for ultrasound applications [41–43], biomicroscopy [44], and dermatologic and ophthalmologic diagnostics [45].

In order to be used for practical energy harvesting purposes, the power output of a PZT transducer must be further improved. Among several types mentioned above, bimorph structure comprising a metal electrode sandwiched between two piezoelectric layers takes much attention due to its capability of energy production with higher density when compared with other types [18, 40, 46–48]. Also, replacing the standard Al electrode used in the bimorph structure with Ag or Pt was shown to affect the energy harvesting performance [36].

In this work, a bimorph fiber composite PZT piezoelectric transducer has been investigated with particular emphasis on its energy harvesting performance. In this respect, the operating conditions for maximizing the electrical signal output have been determined. The quenching of the piezoelectric property with increasing temperature has been demonstrated. Although this material promises high energy yields, it has been shown that the operating conditions to be utilized for different applications must be predetermined with caution since the material exhibits a nonlinear behavior under systematically changing excitations. This behavior is attempted to be interpreted as a result of a change in the resonance frequency at the molecular level for different bending amounts.

2. Materials and Experiments

The fiber composite PZT energy harvester used in this work is schematically depicted in Figure 1. The piezoelectric fibers

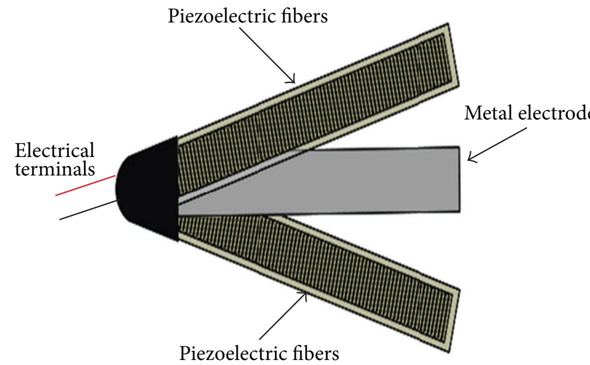

Figure 1: The schematical representation of the bimorph PZT piezoelectric energy harvester used in this work.

were unidirectionally aligned in order to improve both device durability and charge collection efficiency. The electrical signal is observed when the device is flexed, bended, or vibrated. The electrical charges are taken to the battery by the metal electrode spread throughout the midst of the structure. Besides its contribution to the improvement of the charge collection efficiency, this metal electrode helps further prolong the lifetime of the device before it is mechanically broken.

Firstly, the analysis of the voltage signal output of our device was performed before connecting it to rechargeable battery. Figure 2 shows the experimental setup used in this study. The setup was prepared to measure and determine the optimum conditions to obtain maximum electrical energy from the PZT transducer.

In order to gather the experimental data from the device, firstly one of its ends was fixed to a stationary support as shown in Figure 2 since the PZT energy harvester at hand is of flexible type. Then, the device was flexed by a single push and released to let it freely oscillate. The electrical signal was collected by an oscilloscope (Figure 3) for different oscillation frequencies and radii of curvature. Then, it was passed through a data acquisition unit where AC signal produced by the PZT energy harvester was rectified by bridge diodes, filtered by a capacitor, and stored as DC signal. The produced analog voltage value was read by Arduino Mega 2560 microcontroller card and transferred to the data acquiring and analysis model developed by MATLAB/Simulink. Real-time measurement results were recorded by Arduino add-in of MATLAB/Simulink environment.

3. Results and Discussion

3.1. Basic Characteristics. It is seen from the voltage signal in Figure 3 that the first two voltage peaks were more or less spiky. Therefore, we considered the third peak to be V_{max} to render systematic comparisons between different measurements. After the third peak, the decay characteristics of the signal were almost perfectly sinusoidal exhibiting a single period.

The decay kinetics of the oscillations are given in Figure 4. A rapid decay was observed just after the release of the device

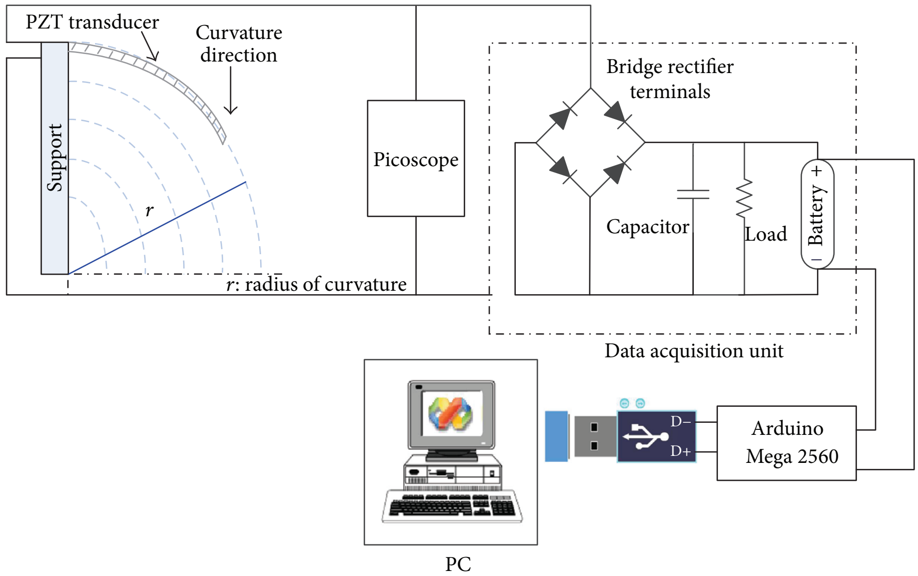

Figure 2: Experimental setup depicting the method of data acquisition from the flexible PZT piezoelectric transducer.

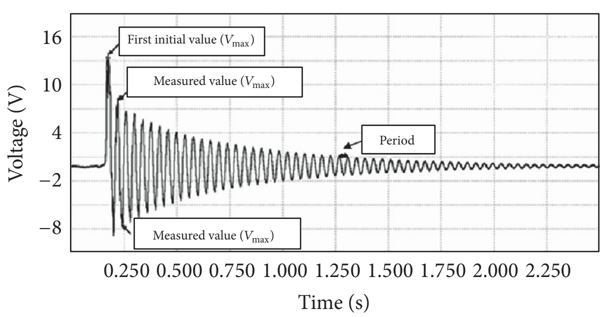

Figure 3: The time dependence of the electrical signal produced by the PZT piezoelectric energy harvester after its release.

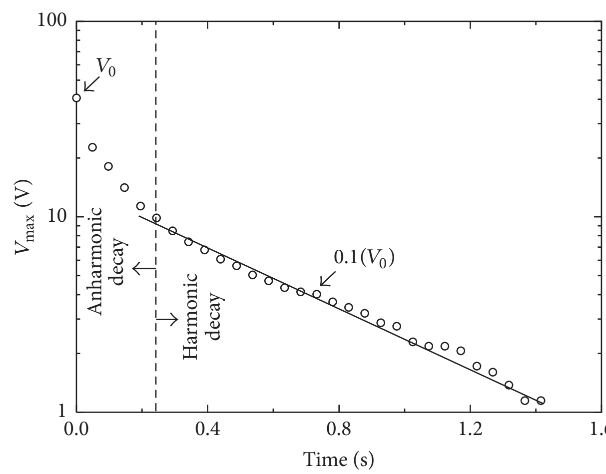

Figure 4: Decay curve of the voltage signal produced by the PZT energy harvester.

during the first oscillations with relatively high amplitudes. At about 0.25 s, this anharmonic behavior is overcome by slower decay characteristics, with the latter being consistent with the simple model of damped harmonic motion. The voltage signal drops down to 10% of V_{max} at ~0.7 s. The damping time of the signal could be increased by connecting a load resistor parallel to the outlet of the rectifier circuit [49]. However, since some portion of the produced power is lost on the load resistor, this method is not preferable despite its contribution to prolong the damping time.

3.2. Length-Frequency Relation. In order to observe the relationship between the length and the frequency of the material, first the length of the material was kept constant and it was observed that the frequency did not change when the material was bent at different ratios. This phenomenon is called the natural frequency of the cantilever [50, 51]. As the material and its mass used in the experiments were not changed, the force applied to change the bending radius did not affect the oscillation frequency which is mainly determined by the inverse proportionality to the length of the PZT cantilever as shown in Figure 5.

3.3. Effect of Temperature on V_{max}. Since the operating temperature of an energy harvester would vary from time to time, the performance of the PZT material at hand was measured at different temperatures. Figure 6 gives the V_{max} value of the material for temperatures ranging from 306 K to 353 K with constant frequency (20 Hz) and bending radius (12 cm). As the operating temperature increases, the voltage output decreases. This behavior is expected due to two main reasons. First, phonons with greater momenta are formed at higher temperatures which results in larger scattering of the free electrons in arbitrary directions reducing their probability of reaching the target electrode. Second, the dielectric function of the PZT material is relaxed at higher temperatures [52],

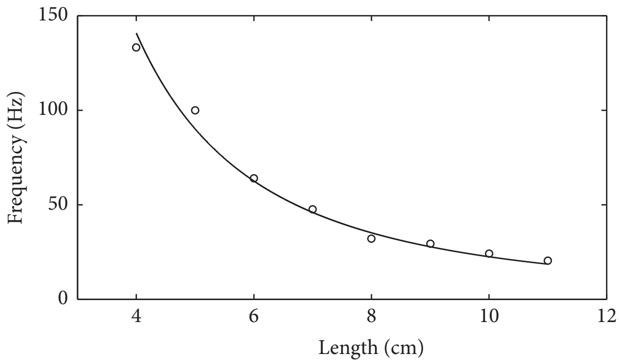

Figure 5: Change of the oscillation frequency with respect to the length of the PZT cantilever.

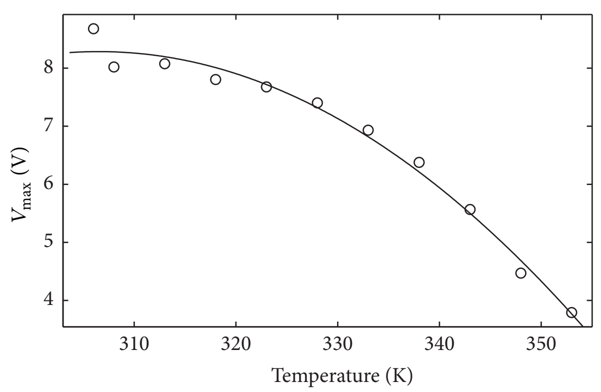

Figure 6: A sample curve showing the monotonously decreasing behavior of V_{max} with increasing temperature. The data were collected at constant frequency of 20 Hz and bending radius of 12 cm.

and after a critical temperature, called the Curie temperature (which is 623 K for this material), the material becomes completely depolarized and loses its piezoelectric properties. For this reason, the operating temperature is advised to be lower than half of the Curie temperature [53–55].

3.4. Frequency Response Characteristics under Stress. The frequency response characteristics of a piezoelectric material are commonly determined by the measurement of the power and/or voltage output signal as a function of the frequency of some external mechanical excitation source. Such measurement methods are usually performed when the piezoelectric material is at rest or under equilibrium. However, in energy harvesting applications, the output signal from the piezoelectric material is collected when it is stressed or out of equilibrium. In this respect, the validity of the standard frequency response curve of a piezoelectric material must be reconsidered if that material is to be used for energy harvesting purposes.

In Figure 7, the mean peak-to-peak voltage output (V_{pp}) per unit length of the PZT energy harvester was recorded as a function of its oscillation frequency at different radii of curvature (r from 9.5 cm to 17.5 cm). Here, inverse of the radius of curvature should be regarded as a degree of strain, distortion, or nonequilibrium.

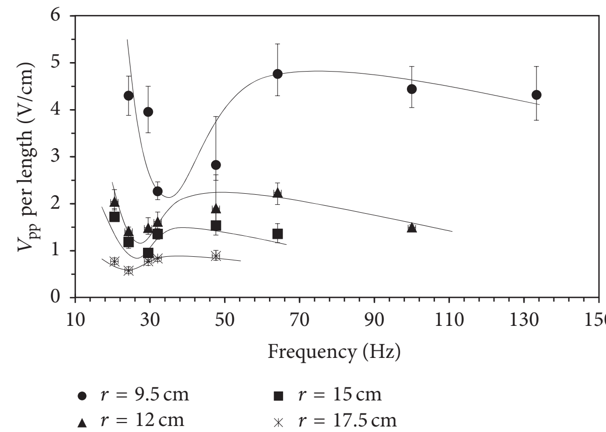

Figure 7: Voltage output per length of the PZT cantilever plotted against oscillation frequency for different radii of curvature. Right shift of the frequency response curve at higher bending amounts is obvious. Solid lines are drawn for eye guide.

For $r = 17.5$ cm, the PZT energy harvester was slightly flexed in reference to its fixing point (see Figure 2 for the experimental setup). It is seen that the voltage output produced by the PZT material first decreases as the oscillation frequency increases from 20 Hz to 23 Hz. As the frequency is further increased toward 30 Hz, the voltage output starts to increase and finally passes over a maximum at about 33 Hz (note here that this frequency is in good agreement with the common resonance frequency of that material measured with direct external mechanical excitation while the material is kept at rest). The voltage signal slowly decreases for higher frequencies. This "spoon-like" behavior is common for all measurement sets. The behavior around the minimum point in this curve seems to be related to the absorption of the vibrational energy and its subsequent dissipation as phonons throughout the structure without the production of any electrical signal. On the other hand, the behavior around the maximum is directly related to the conversion of the vibrational energy into the electrical energy by the matching of the oscillation frequency with the molecular resonance frequency (i.e., the vibrational frequency becomes some integer multiple of the molecular resonance frequency which leads to a constructive effect and boosts the polarization of the PZT molecules). Interestingly, this characteristic curve shifts to higher frequencies at lower radii of curvature (i.e., stronger bending). In other words, together with an increase in the maximum voltage output, the oscillation frequency at which this voltage output is reached also increases. It should be noted here that the characteristic "spoon-like" curve upshifts as a whole in the frequency axis at different radii of curvature; that is, the frequency corresponding to the minimum voltage also shifts in the same manner. However, assuming that the underlying reason for the upshift of the curves remains the same, a physical interpretation is proposed focusing on the frequency shift of only the "maximum" voltage output which is the relevant quantity for an energy harvester.

3.5. Interpretation of the Shift of the Resonance Frequency. To start with, the Morse Potential is taken as the interatomic interaction energy, U, between the constituent atoms of the PZT structure:

$$U \propto \left(1 - \exp\left[-\beta\left(r - r_c\right)\right]\right)^2. \tag{1}$$

Here, β is a parameter related to the width of the potential well and r_c is the equilibrium distance between two subsequent atoms. Although Hooke's Law gives exact analytical solution to Schrödinger's Equation in the simple model of quantum harmonic oscillator, Morse's Law is more general as it takes both the anharmonicity and the overtone transitions into account. Indeed, Hooke's Law is the second-order Taylor expansion of (1) and therefore can be assumed to be a simplified version of Morse's Law.

Within the frame of the physical principles, the upshift of the resonance frequency with increasing initial bending must be related to an increase in the β factor in (1). Two of the possibilities for β to take different values at different bending amounts are discussed in the following two subsections.

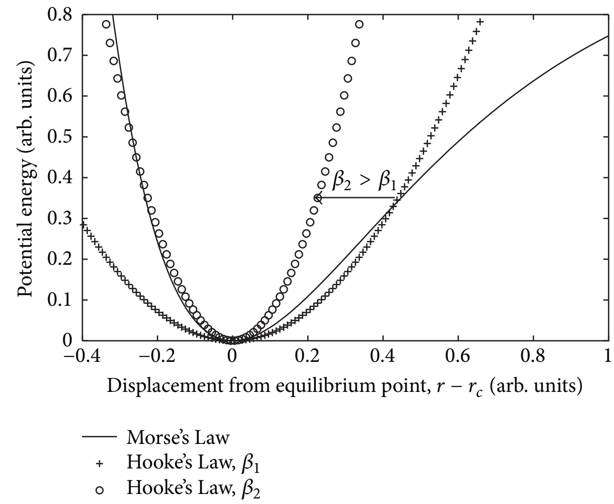

FIGURE 8: Potential energy curves plotted with Morse's and Hooke's Laws. A possible overtone transition from a lower to higher β mode is shown by the arrow.

3.5.1. What Happens in the Vicinity of the Elastic/Plastic Deformation Regions? Note that β is directly proportional to the modulus of elasticity, which is defined as the slope of the stress-to-strain curve in the elastic deformation region. The slope of that curve decreases at larger strain values and finally becomes zero where the material reaches its ultimate strength. In other words, a material starts to lose its ability to restore its original shape with increasing bending amounts and, after a critical point, the type of deformation changes from elastic to plastic. From microscopic point of view, some of the atomic bonds start to form defect states leading to a lower restoring force. Such behavior results in a decrease in β, and therefore it cannot be attributed to the phenomena observed in this work. Here, the previous works [56, 57] on piezoelectric MEMS reporting a decrease in the resonance frequency at higher acceleration values should not be confused since the concept of resonance frequency of those works was used for the oscillation frequency determined by the dimensions of the MEMS cantilever whose length-to-volume ratio is much larger. Probably, their piezoelectric cantilever experiences a more or less prominent nonlinear stress-to-strain curve. On the contrary, the resonance frequency in this work corresponds to the oscillations in the molecular level.

3.5.2. Overtone Transitions to a Stiffer Mode. Although the experiments on the material of this work were performed with initial elastic deformation, the degree of anharmonicity increases with increasing bending according to (1) (Figure 8). For the correct interpretation of the increase in the resonance frequency with increasing bending, the dynamics at the very moment of the release are crucial since V_{pp} is determined from the second sine-wave of the oscillations. It is seen in Figure 4 that the PZT transducer firstly experiences a fast anharmonic decay; then a transition to a relatively slow harmonic decay occurs. The decay of the output voltage is a direct result of the decrease in the oscillation amplitude $r - r_c$ in (1). On the other hand, it should be kept in mind that the overall energy loss is mainly governed by possible phonon emission mechanisms where the temperature has a key role (Figure 6). Considering the constant temperature (i.e., room temperature) for all sets of measurements in Figure 7, no drastic change is expected in the main energy loss mechanism. In this regard, the decrease in the oscillation amplitude during the fast anharmonic decay just after the release cannot be totally attributed to the potential energy loss in the material. Instead, during the strong attempt to rearrange its oscillation behavior (i.e., from anharmonic to harmonic), the PZT material can make an overtone transition from a lower β state toward a higher β state. One of the underlying reasons for this strong attempt may be the instability imposed by the inequality between the repulsive force applied on the compressed half and the attractive force applied on the expanded half of the flexed material during an anharmonic oscillation. Regarding the conservation of energy arguments, such a transition is possible as shown in Figure 8. When the material is excited by bending, Morse's curve in Figure 8 might be followed. The PZT material having such a potential curve can be said to be in a relatively lower β state as designated by the corresponding Hooke's curve with β_1. Assuming an instantaneous rearrangement just after the release, the PZT material can transit to Hooke's curve with β_2, where $\beta_2 > \beta_1$. This assumption seems to be reasonable due to its good agreement with the "quick" transition from the anharmonic to the harmonic state. Obviously, at higher bending amounts, the material experiences a larger restoring force and consequently a faster anharmonic-to-harmonic transition leading to a greater difference $\beta_2 - \beta_1$ and to a greater upshift of the resonance frequency.

3.6. Storage of the Electrical Energy. Besides extracting the maximum possible output voltage from the PZT material at hand, storing that voltage with minimum losses is also

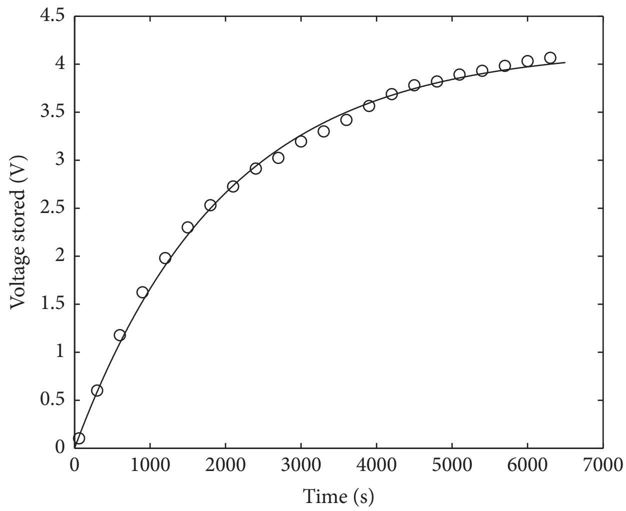

Figure 9: Charge storage characteristics of the PZT energy harvester measured at the optimum operating conditions.

important. One of the efficient ways is that the sinusoidal electrical signal can be passed through a rectifying circuit and filtered before its storage in a battery (Figure 2). Then, the stored energy would be ready to use at any time for any purposes. Figure 9 shows the time dependence of the stored voltage in a 0.1 F capacitor at an oscillation frequency of 20 Hz with bending radius of curvature of 9.5 cm. These parameters may be regarded as the optimum operating conditions for this PZT piezoelectric energy harvester. Another set of parameters for maximum voltage output would be formed by using 65 Hz as the oscillation frequency instead of 20 Hz (Figure 7). However, this would mean at least three times more frequent oscillations of a stiffer material at a large bending and, therefore, would not be a good choice in order to avoid faster fatigue and lower lifetime of the material. With the determined optimum operating conditions, the amount of energy stored in 6300 s at room temperature is 0.8 J. The maximum voltage output observed at the instant of the release under optimum conditions was slightly more than 200 V and the current at this high voltage was 53 μA which results in a power of about 10 mW.

4. Conclusion

In this study, the energy production capability of fiber reinforced bimorph PZT piezoelectric transducer was examined systematically. The electrical signal was collected by a high yield energy harvester circuitry during the self-oscillations of the PZT material after an externally applied bending. The sinusoidal voltage signal created by the mechanical oscillations exhibited an initial fast anharmonic decay followed by a relatively slower harmonic decay. The frequency of these oscillations could be adjusted by changing the length of the piezoelectric cantilever. The ambient temperature, which is crucial especially for outdoor energy harvesting applications, has a strong effect on the produced electrical signal. It is advised that the temperature of the PZT material should not exceed half of the Curie temperature in order to keep the phonon scattering and the dielectric relaxation at low levels. The frequency response curve shows an upshift in the frequency axis with increasing bending amounts. Regarding the energy conservation principle, this behavior was attributed to an increase in the β factor of the PZT material in the form of a transition to a stiffer oscillation mode. The optimum room temperature operating conditions of the PZT energy harvester at hand were determined to be 20 Hz oscillation frequency and 9.5 cm radius of curvature. At these optimum conditions, the maximum voltage ($V_{\max}$) and the corresponding electrical current obtained are around 200 V and 53 μA, respectively, producing an electrical power of about 10 mW. Although this power level seems to be low compared to the conventional renewable energy systems, it was obtained from a single PZT material and can be boosted by a proper configuration including multiple number of PZT materials. Also, such power levels in the order of milliwatts are sufficient for applications such as biosensing, MEMS thermal imaging, and wireless network systems.

Competing Interests

The authors declare that they have no competing interests.

References

[1] T. Starner, “Human-powered wearable computing,” *IBM Systems Journal*, vol. 35, no. 3-4, pp. 618–629, 1996.

[2] R. Amirtharajah and A. P. Chandrakasan, “Self-powered signal processing using vibration-based power generation,” *IEEE Journal of Solid-State Circuits*, vol. 33, no. 5, pp. 687–695, 1998.

[3] S. Roundy, P. K. Wright, and J. Rabaey, “A study of low level vibrations as a power source for wireless sensor nodes,” *Computer Communications*, vol. 26, no. 11, pp. 1131–1144, 2003.

[4] S. P. Beeby, M. J. Tudor, and N. M. White, “Energy harvesting vibration sources for microsystems applications,” *Measurement Science and Technology*, vol. 17, no. 12, pp. R175–R195, 2006.

[5] J. C. Park and J. Y. Park, “Asymmetric PZT bimorph cantilever for multi-dimensional ambient vibration harvesting,” *Ceramics International*, vol. 39, no. 1, pp. S653–S657, 2013.

[6] D.-J. Shina, S.-J. Jeongb, C.-E. Seoc, K.-H. Choc, and J.-H. Koh, “Multi-layered piezoelectric energy harvesters based on PZT ceramic actuators,” *Ceramics International*, vol. 41, supplement 1, pp. 686–690, 2005.

[7] S. R. Platt, S. Farritor, and H. Haider, “On low-frequency electric power generation with PZT,” *IEEE/ASME Transactions on Mechatronics*, vol. 10, no. 2, pp. 240–252, 2005.

[8] P. D. Mitcheson, E. K. Reilly, T. Toh, P. K. Wright, and E. M. Yeatman, “Performance limits of the three MEMS inertial energy generator transduction types,” *Journal of Micromechanics and Microengineering*, vol. 17, no. 9, pp. S211–S216, 2007.

[9] S. R. Anton and H. A. Sodano, “A review of power harvesting using piezoelectric materials (2003–2006),” *Smart Materials and Structures*, vol. 16, no. 3, pp. R1–R21, 2007.

[10] R. Torah, P. Glynne-Jones, M. Tudor, T. O’Donnell, S. Roy, and S. Beeby, “Self-powered autonomous wireless sensor node using vibration energy harvesting,” *Measurement Science and Technology*, vol. 19, no. 12, Article ID 125202, 2008.

[11] D.-J. Shin, W.-S. Kang, J.-H. Koh, K.-H. Cho, C.-E. Seo, and S.-K. Lee, “Comparative study between the pillar- and bulk-type multilayer structures for piezoelectric energy harvesters,” *Physica Status Solidi (A) Applications and Materials Science*, vol. 211, no. 8, pp. 1812–1817, 2014.

[12] P. Janphuang, R. Lockhart, N. Uffer, D. Briand, and N. F. De Rooij, “Vibrational piezoelectric energy harvesters based on thinned bulk PZT sheets fabricated at the wafer level,” *Sensors and Actuators A: Physical*, vol. 210, pp. 1–9, 2014.

[13] N. S. Hudak and G. G. Amatucci, “Small-scale energy harvesting through thermoelectric, vibration, and radiofrequency power conversion,” *Journal of Applied Physics*, vol. 103, no. 10, Article ID 101301, 2008.

[14] D. Shen, J.-H. Park, J. H. Noh et al., “Micromachined PZT cantilever based on SOI structure for low frequency vibration energy harvesting,” *Sensors and Actuators, A: Physical*, vol. 154, no. 1, pp. 103–108, 2009.

[15] H. A. Sodano, D. J. Inman, and G. Park, “Comparison of piezoelectric energy harvesting devices for recharging batteries,” *Journal of Intelligent Material Systems and Structures*, vol. 16, no. 10, pp. 799–807, 2005.

[16] A. Abdullah, M. Shahini, and A. Pak, “An approach to design a high power piezoelectric ultrasonic transducer,” *Journal of Electroceramics*, vol. 22, no. 4, pp. 369–382, 2009.

[17] S. Priya, “Advances in energy harvesting using low profile piezoelectric transducers,” *Journal of Electroceramics*, vol. 19, no. 1, pp. 165–182, 2007.

[18] C. Fei, Z. Chen, W. M. Fong et al., “Modification of microstructure on PZT films for ultrahigh frequency transducer,” *Ceramics International*, vol. 41, no. 1, pp. S650–S655, 2015.

[19] D. Wang, E. Filoux, F. Levassort, M. Lethiecq, S. A. Rocks, and R. A. Dorey, “Fabrication and characterization of annular-array, high-frequency, ultrasonic transducers based on PZT thick film,” *Sensors and Actuators A: Physical*, vol. 216, no. 1, pp. 207–213, 2014.

[20] G. R. Lockwood, D. H. Turnbull, D. A. Christopher, and F. S. Foster, “Beyond 30 MHz applications of high frequency ultrasound imaging,” *IEEE Engineering in Medicine and Biology Magazine*, vol. 15, no. 6, pp. 60–71, 1996.

[21] C. Luo, G. Z. Cao, and I. Y. Shen, “Development of a lead-zirconate-titanate (PZT) thin-film microactuator probe for intracochlear applications,” *Sensors and Actuators, A: Physical*, vol. 201, pp. 1–9, 2013.

[22] C. D. Liaoand and J. C. Tsai, “The evolution of MEMS displays,” *IEEE Transactions on Industrial Electronics*, vol. 56, no. 4, pp. 1057–1065, 2009.

[23] K. H. Koh, T. Kobayashi, and C. Lee, “Investigation of piezoelectric driven MEMS mirrors based on single and double S-shaped PZT actuator for 2-D scanning applications,” *Sensors and Actuators A: Physical*, vol. 184, pp. 149–159, 2012.

[24] C. Lee and J. A. Yeh, “Development and evolution of MOEMS technology in variable optical attenuators,” *Journal of Microlithography Microfabrication and Microsystems*, vol. 7, no. 2, Article ID 021003, 2008.

[25] C. Lee, F.-L. Hsiao, T. Kobayashi et al., “A 1-V operated MEMS variable optical attenuator using piezoelectric PZT thin-film actuators,” *IEEE Journal on Selected Topics in Quantum Electronics*, vol. 15, no. 5, pp. 1529–1536, 2009.

[26] K. H. Koh, C. Lee, and T. Kobayashi, “A piezoelectric-driven three-dimensional MEMS VOA using attenuation mechanism with combination of rotational and translational effects,” *Journal of Microelectromechanical Systems*, vol. 19, no. 6, Article ID 5597910, pp. 1370–1379, 2010.

[27] J. A. Yeh, S.-S. Jiang, and C. Lee, “MOEMS variable optical attenuators using rotary comb drive actuators,” *IEEE Photonics Technology Letters*, vol. 18, no. 10, pp. 1170–1172, 2006.

[28] R. F. Wolffenbuttel, “MEMS-based optical mini- and microspectrometers for the visible and infrared spectral range,” *Journal of Micromechanics and Microengineering*, vol. 15, no. 7, pp. 145–152, 2005.

[29] J. S. Milne, J. M. Dell, A. J. Keating, and L. Faraone, “Widely tunable MEMS-based Fabry-Perot filter,” *Journal of Microelectromechanical Systems*, vol. 18, no. 4, pp. 905–913, 2009.

[30] N. Neumann, M. Ebermann, S. Kurth, and K. Hiller, “Tunable infrared detector with integrated micromachined Fabry-Perot filter,” *Journal of Micro/Nanolithography, MEMS, and MOEMS*, vol. 7, no. 2, Article ID 021004, 2008.

[31] J. Sun, S. Guo, L. Wu et al., “3D *in vivo* optical coherence tomography based on a low-voltage, large-scan-range 2D MEMS mirror,” *Optics Express*, vol. 18, no. 12, pp. 12065–12075, 2010.

[32] T.-H. Tsai, B. Potsaid, M. F. Kraus et al., “Piezoelectric-transducer-based miniature catheter for ultrahigh-speed endoscopic optical coherence tomography,” *Biomedical Optics Express*, vol. 2, no. 8, pp. 2438–2448, 2011.

[33] Y. Wang, M. Raj, H. S. McGuff et al., “Portable oral cancer detection using a miniature confocal imaging probe with a large field of view,” *Journal of Micromechanics and Microengineering*, vol. 22, no. 6, Article ID 065001, 2012.

[34] Y. Xu, J. Singh, C. S. Premachandran et al., “Design and development of a 3D scanning MEMS OCT probe using a novel SiOB package assembly,” *Journal of Micromechanics and Microengineering*, vol. 18, no. 12, Article ID 125005, 2008.

[35] A. D. Aguirre, P. R. Herz, Y. Chen et al., “Two-axis MEMS scanning catheter for ultrahigh resolution three-dimensional and En face imaging,” *Optics Express*, vol. 15, no. 5, pp. 2445–2453, 2007.

[36] H. L. Zhang, J.-F. Li, B.-P. Zhang, and W. Jiang, “Enhanced mechanical properties in Ag-particle-dispersed PZT piezoelectric composites for actuator applications,” *Materials Science and Engineering: A*, vol. 498, no. 1-2, pp. 272–277, 2008.

[37] S. W. Shin and T. K. Oh, “Application of electro-mechanical impedance sensing technique for online monitoring of strength development in concrete using smart PZT patches,” *Construction and Building Materials*, vol. 23, no. 2, pp. 1185–1188, 2009.

[38] D. F. Wang, X. Li, J. Lu, T. Sagawa, and R. Maeda, “Ring-shaped PZT film resonator for bio-sensing applications in liquid environment,” *Procedia Engineering*, vol. 25, pp. 443–446, 2011.

[39] H. J. Zhao, T. L. Ren, N. X. Zhang et al., “High-frequency properties of PZT for RF-communication applications,” *Materials Science and Engineering: B*, vol. 99, no. 1–3, pp. 192–194, 2003.

[40] J. Ou-Yang, B. Zhu, X. Yan, J. Zhao, W. Ren, and X. Yang, “Electrical properties of PMN-PZT film on silicon lens,” *Ceramics International*, vol. 41, no. 3, pp. 4243–4247, 2015.

[41] X. Chen, C. Fei, Z. Chen et al., “Simulation and fabrication of 0–3 composite PZT films for ultrahigh frequency (100–300 MHz) ultrasonic transducers,” *Journal of Applied Physics*, vol. 119, no. 9, Article ID 094103, 2016.

[42] D.-W. Wu, Q. Zhou, X. Geng, C.-G. Liu, F. Djuth, and K. K. Shung, “Very high frequency (beyond 100 MHz) PZT kerfless linear arrays,” *IEEE Transactions on Ultrasonics, Ferroelectrics, and Frequency Control*, vol. 56, no. 10, pp. 2304–2310, 2009.

[43] W. Dawei, *Development of High-Frequency (~ 100MHz) PZT Thick-Film Ultrasound Transducers and Arrays*, University of California, 2009.

[44] M. Lukacs, M. Sayer, D. Knapic, R. Candel, and F. S. Foster, "Novel PZT films for ultrasound biomicroscopy," in *Proceedings of the IEEE Ultrasonics Symposium*, vol. 2, pp. 901–904, San Antonio, Tex, USA, November 1996.

[45] C. Passman and E. Helmut, "A 100-MHz ultrasound imaging system for dermatologic and opthmologic diagnostic," *IEEE Transactions on Ultrosonics, Ferroelectrics and Frequency Control*, vol. 43, no. 4, pp. 545–552, 2016.

[46] H. Kueppers, T. Leuerer, U. Schnakenberg et al., "PZT thin films for piezoelectric microactuator applications," *Sensors and Actuators, A: Physical*, vol. 97-98, pp. 680–684, 2002.

[47] D. Isarakorn, D. Briand, A. Sambri et al., "Finite element analysis and experiments on a silicon membrane actuated by an epitaxial PZT thin film for localized-mass sensing applications," *Sensors and Actuators B: Chemical*, vol. 153, no. 1, pp. 54–63, 2011.

[48] M. R. Mohammadi, S. A. Tabei, A. Nemati, D. Eder, and T. Pradeep, "Synthesis and crystallization of lead-zirconium-titanate (PZT) nanotubes at the low temperature using carbon nanotubes (CNTs) as sacrificial templates," *Advanced Powder Technology*, vol. 23, no. 5, pp. 647–654, 2012.

[49] H. A. Sodano, G. Parkand, and D. J. Inman, "Estimation of electric charge output for piezoelectric energy harvesting," *Strain Journal*, vol. 40, no. 2, pp. 49–58, 2004.

[50] K. Junwu, Y. Zhigang, P. Taijiang, C. Guangming, and W. Boda, "Design and test of a high-performance piezoelectric micropump for drug delivery," *Sensors and Actuators A: Physical*, vol. 121, no. 1, pp. 156–161, 2005.

[51] H. Fang, J. Liu, Z. Xu, L. Dong, L. Wang, and D. Chen, "Fabrication and performance of MEMS-based piezoelectric power generator for vibration energy harvesting," *Microelectronics Journal*, vol. 37, no. 11, 2006.

[52] F. Levassort, P. Tran-Huu-Hue, E. Ringaard, and M. Lethiecq, "High-frequency and high-temperature electromechanical performances of new PZT-PNN piezoceramics," *Journal of the European Ceramic Society*, vol. 21, no. 10-11, pp. 1361–1365, 2001.

[53] C. Miclea, C. Tanasoiu, L. Amarande et al., "Temperature dependence of the main piezoelectric parameters of a Nb-Li doped PZT ceramic," in *Proceedings of the International Semiconductor Conference (CAS '06)*, pp. 279–282, IEEE, September 2007.

[54] H. Kungl and M. J. Hoffmann, "Temperature dependence of poling strain and strain under high electric fields in LaSr-doped morphotropic PZT and its relation to changes in structural characteristics," *Acta Materialia*, vol. 55, no. 17, pp. 5780–5791, 2007.

[55] X. X. Wang, K. Murakami, O. Sugiyama, and S. Kaneko, "Piezoelectric properties, densification behavior and microstructural evolution of low temperature sintered PZT ceramics with sintering aids," *Journal of the European Ceramic Society*, vol. 21, no. 10-11, pp. 1367–1370, 2001.

[56] S. N. Chen, G. J. Wang, and M. C. Chien, "Analytical modeling of piezoelectric vibration-induced micro power generator," *Mechatronics*, vol. 16, no. 7, pp. 379–387, 2006.

[57] J. W. Yi, W. Y. Shih, and W.-H. Shih, "Effect of length, width, and mode on the mass detection sensitivity of piezoelectric unimorph cantilevers," *Journal of Applied Physics*, vol. 91, no. 3, pp. 1680–1686, 2002.